ADVANCED MATERIALS

[6] G. Yu, J. Gao, J. C. Hummelen, F. Wudl, A. J. Heeger, *Science* **1995**, *270*, 1789.
[7] C. J. Drury, C. M. J. Mutsaers, C. M. Hart, M. Matters, D. M. de Leeuw, *Appl. Phys. Lett.* **1998**, *73*, 108.
[8] T. R. Hebner, C. C. Wu, D. Marcy, M. H. Lu, J. C. Sturm, *Appl. Phys. Lett.* **1998**, *72*, 519.
[9] E. Sachs, M. Cima, J. Bredt, A. Curodeau, T. Fan, D. Brancazio, *Manufact. Rev.* **1992**, *5*, 117.
[10] J. Bharathan, Y. Yang, *Appl. Phys. Lett.* **1998**, *72*, 2660; S. C. Chang, J. Bharathan, Y. Yang, R. Helgeson, F. Wudl, M. B. Ramey, J. R. Reynolds, *Appl. Phys. Lett.* **1998**, *73*, 2561.
[11] K. Gilleo, *Polymer Thick Films,* Van Nostrand Reinhold, New York, **1996**.
[12] Z. Bao, Y. Feng, A. Dodabalapur, V. R. Raju, A. J. Lovinger, *Chem. Mater.* **1997**, *9*, 1299.
[13] F. Garnier, R. Hajlaoui, A. Yasser, P. Srivastava, *Science* **1994**, *265*, 1684.
[14] E. Kim, Y. Xia, G. M. Whitesides, *Nature* **1995**, *376*, 581.
[15] J. A. Rogers, Z. Bao, V. R. Raju, *Appl. Phys. Lett.* **1998**, *72*, 2716.
[16] A. Kumar, G. M. Whitesides, *Appl. Phys. Lett.* **1993**, *63*, 2002.
[17] D. Qin, Y. Xia, J. A. Rogers, R. J. Jackman, X. M. Zhao, G. M. Whitesides, in *Microsystem Technology in Chemistry and Life Science*, (Eds: A. Manz, H. Becker), Topics in Current Chemistry, Vol. 194, Springer, Berlin, **1998**, pp. 1–20.
[18] Y. Xia, G. M. Whitesides, *Angew. Chem. Int. Ed.* **1998**, *37*, 550.
[19] J. L. Wilbur, A. Kumar, E. Kim, G. M. Whitesides, *Adv. Mater.* **1994**, *6*, 600; Y. Xia, X. M. Zhao, E. Kim, G. M. Whitesides, *Chem. Mater.* **1995**, *7*, 2332.
[20] Y. Xia, E. Kim, G. M. Whitesides, *J. Electrochem. Soc.* **1996**, *143*, 1070.
[21] H. A. Biebuyck, N. B. Larsen, E. Delamarche, B. Michel, *IBM J. Res. Develop.* **1997**, *41*, 159.
[22] X. M. Zhao, J. L. Wilbur, G. M. Whitesides, *Langmuir* **1996**, 12, 3257.
[23] E. Delamarche, B. Michel, H. Kang, C. Gerber, *Langmuir* **1994**, *10*, 4103.
[24] J. Huang, J. C. Hemminger, *J. Am. Chem. Soc.* **1993**, *115*, 3342.
[25] Z. Bao, A. Dodabalapur, A. J. Lovinger, *Appl. Phys. Lett.* **1996**, *69*, 4108.
[26] O. J. A. Schueller, D. C. Duffy, J. A. Rogers, S. T. Brittain, G. M. Whitesides, *Sens. Actuat. A*, in press.
[27] Y. Xia, D. Qin, G. M. Whitesides, *Adv. Mater.* **1996**, *8*, 1015.
[28] J. A. Rogers, K. E. Paul, G. M. Whitesides, *JVST B* **1998**, *16*, 88.

For ordering information see p. 701

Oblique Incidence Organic Molecular Beam Deposition and Nonlinear Optical Properties of Organic Thin Films with a Stable In-Plane Directional Order**

By *Chengzhi Cai*, *Martin M. Bösch*, *Bert Müller*, *Ye Tao*, *Armin Kündig*, *Christian Bosshard*,* *Zhehong Gan*, *Ivan Biaggio*, *Ilias Liakatas*, *Matthias Jäger*, *Hansjörg Schwer*, and *Peter Günter*

Organic thin films with non-centrosymmetric ordering of dipoles are very attractive as waveguides for nonlinear optic and electro-optic applications.[1,2] High electric field poling or self-assembly has been widely used to align dipolar molecules perpendicular to the film surface.[2] However, only a few examples of in-plane alignment of dipolar molecules have been described, including epitaxy on a lattice-matched organic substrate surface,[3,4] in-plane poling,[5] and Langmuir–Blodgett film deposition.[6,7] Based on a new type of nonlinear optical material, we have demonstrated, to our knowledge for the first time, that the dipolar molecules in an organic thin film can be in-situ aligned in any desired direction within the film plane by organic molecular beam deposition (OMBD) at oblique incidence.[8] This one-component, relatively fast (5 nm min^{-1}), OMBD based, and easily controlled thin film growth technique provides a new tool for the production of organic thin films with an in-plane directional order for second-order nonlinear optics (NLO) and electro-optics.

Growth of organic thin films by OMBD (Fig. 1A) in ultrahigh vacuum (UHV) has many advantages over solution-based techniques,[9,10] such as greatly reduced contamination in the UHV environment, in-situ growth monitoring, high density of chromophores, and reasonably high growth rate. In addition, mask-defined microstructures such as strip waveguides, and integrated hetero-layer structures, like light emitting diode (LED) devices,[8,11] can be fabricated by OMBD. Despite these advantages, OMBD is still much less developed as compared to solution-based techniques for the preparation of second-order NLO films. The main obstacle lies within the materials.

[*] Dr. C. Bosshard, Dr. C. Cai, M. M. Bösch, Dr. B. Müller[+], Dr. Y. Tao, A. Kündig, Dr. I. Biaggio, I. Liakatas, Dr. M. Jäger, Prof. P. Günter
Nonlinear Optics Laboratory, Institute of Quantum Electronics
Swiss Federal Institute of Technology
ETH Hönggerberg, CH-8093 Zürich (Switzerland)
Dr. Z. Gan
Laboratory of Physical Chemistry, Department of Chemistry
Swiss Federal Institute of Technology
ETH Zentrum, CH-8092 Zürich (Switzerland)
Dr. H. Schwer
Laboratory for Solid State Physics
ETH Hönggerberg, CH-8093 Zürich (Switzerland)
[+] Present address: Swiss Federal Laboratories for Materials Testing and Research, CH-8600 Dübendorf, Switzerland.
[**] Financial support from the Swiss Priority Program Optique II is gratefully acknowledged. We thank Mr. P. Wägli for the SEM measurements.

  0935-9648/99/0906-0745 $ 17.50+.50/0

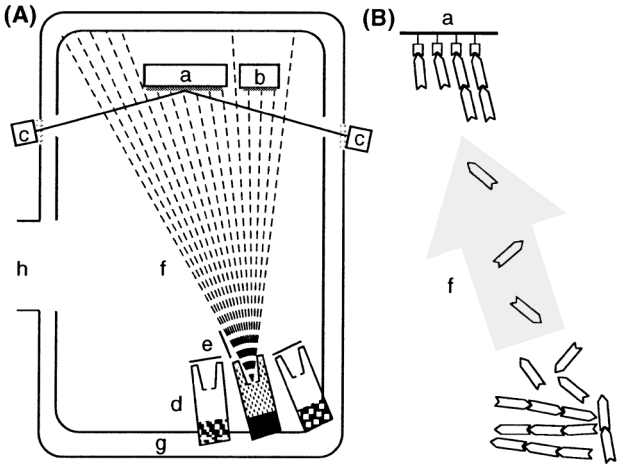

Fig. 1. (A) Illustration of OMBD. An organic thin film on the substrate (a) is growing out of the molecular beam (f), formed by evaporating the material from the effusion cell (d) into the chamber in UHV ($< 10^{-8}$ mbar), which is generated by a turbo molecular pump (h) and a liquid nitrogen shroud (g). The growth rate and film thickness are monitored in situ with monolayer sensitivity by the quartz crystal thickness monitor (b) and the ellipsometer (c). The deposition (on/off) is controlled by the shutter (e). In our home-made OMBD chamber, the distance between beam source and substrate is 26 cm. The incident (deposition) angle, defined as the angle between the molecular beam and substrate surface normal, is about 26°. (B) Illustration of the self-assembly growth of ordered thin films. At elevated temperatures, the supramolecular polymer (bottom) is degraded into the monomers, which are emitted into the UHV chamber to form a molecular beam (f), and deposited on the substrate surface (a) where they polymerize again in a head-to-tail arrangement, directed by the substrate surfaces.

So far, organic NLO-active materials can be divided into low molecular weight organic crystals and amorphous polymers.[1,2] Only the former are OMBD compatible. However, single crystalline films with a large area and a useful thickness are extremely difficult to grow, and crystalline films are usually composed of micrometer-sized crystallites, which lead to large scattering losses.[5] On the other hand, amorphous films with no crystallites or with crystallites of a size smaller than about 100 nm do not have this drawback, and they are much easier to grow by OMBD. Nevertheless, although amorphous low molecular weight materials have been widely used in LED devices,[11,12] to the best of our knowledge, they have not been reported for use in second-order nonlinear optics. This may be due to the difficulties in designing the materials, which should be at least: (i) OMBD compatible with a proper vapor pressure and high thermal stability; (ii) able to self-assemble non-centrosymmetrically; (iii) amorphous or having low scattering losses; (iv) highly stable against orientational randomization.

To meet these requirements, we propose to use dipolar chromophores, which form strong head-to-tail intermolecular hydrogen bonds, thereby forming linear supramolecular assemblies[13,14] in the solid state. If the strong hydrogen bonds that link the monomers can be broken while the monomers are intact at evaporation temperatures, it is possible to sublimate such supramolecular polymers in ultrahigh vacuum. This is in contrast to traditional polymers in which monomeric units are covalently bonded. The sublimated monomers are then deposited on the substrate surface where they polymerize again in a head-to-tail fashion (Fig. 1B). A substrate surface that selectively bonds only one end of the molecules is used to orient each polymer chain in the same direction, forming a directional ordered supramolecular polymer film. Microphase separation through crystallization in such supramolecular polymers is expected to be greatly reduced by the directionality of the strong hydrogen bonding.[14] Formation of a strong hydrogen bond network in the material should also lower the vapor pressure, and stabilize the structural order of the material.

To explore the feasibility of the idea discussed above, 4-[*trans*-(pyridin-4-ylvinyl)]benzoic acid (**1**) and 4-(pyridin-4-ylethynyl)benzoic acid (**2**) were selected as model compounds. They are unlikely to display a high nonlinearity because of the absence of strong donor/acceptor substituents. However, they have a rigid and linear molecular structure. Accordingly, the possibility of individual molecules adopting differently bent conformations, which complicates the supramolecular structural analysis of the materials, is negligible for **1** and **2**. In addition, **1** and **2** are expected to form strong intermolecular head-to-tail hydrogen bonds (COOH···N) in the solid state.[15] Therefore, they are suitable materials for preliminary experiments. We have shown that films of **2** grown on amorphous glass substrates have an in-plane order with a direction parallel to the projection of the molecular beam direction on the substrate surface.[16] In this and the subsequent paper, we report the results of using **1** as the film material. The melting point of **1** (350 °C) is significantly higher than that of **2** (300 °C). This may lead to a higher thermal stability against orientational randomization for films of **1** than **2**. A practical reason for using **1** instead of **2** is the availability: many grams of **1** can be prepared easily in one step (93 % yield) from cheap commercially available materials, while four laborious steps (55 % overall yield) are required to prepare **2**.

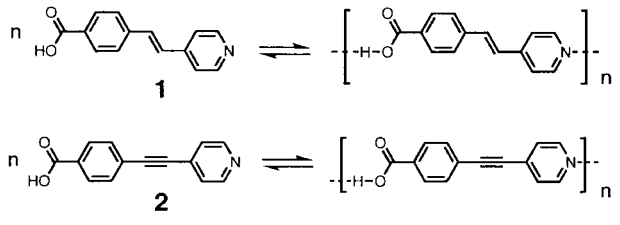

The strong head-to-tail hydrogen bonding (COOH···N) in the solid state of **1** and **2** was indicated by solid state ^{15}N NMR spectroscopy.[16–18] The only ^{15}N signals of **1** and **2** appear at –106 and –105 p.p.m. relative to that of $CH_3{}^{15}NO_2$ (0 p.p.m.), while that of the methyl ester of **2** is at –67 p.p.m. The large upfield shift (about 40 p.p.m.) of the acid as compared to that of the ester is not due to the substituent effect,[19] but to strong hydrogen bonding on the nitrogen atom (COOH···N). In addition, low molecular weight **1** melts at 350 °C, dramatically higher than the melting point (105–107 °C) of its methyl ester where the –OH group in **1**

0935-9648/99/0906-0746 $ 17.50+.50/0

ADVANCED MATERIALS

is replaced with $-OCH_3$, which prevents hydrogen bond formation. In addition, the material is insoluble in common organic solvents at room temperature. On the other hand, powder of **1** became slightly soluble in hot DMSO, and sublimated at 200 °C and 0.01 mbar, indicating that the hydrogen bond network can be broken at elevated temperatures. ^{1}H NMR and mass spectra of the sublimated materials confirmed that molecules of **1** were intact after sublimation. SHG powder tests[20] of the sublimated powder of **1** at λ_0 = 1.3 μm showed a second harmonic light intensity comparable to that of a urea standard, suggesting a non-centrosymmetric order of the molecules in the powder.

Films of **1** with a thickness of 100–400 nm were deposited on amorphous glass substrates by OMBD (Fig. 1A). The substrates are made of amorphous glass (microscope slides, 2 × 2 cm^2). The cleaning procedure was simple: we immersed the substrates in an ultrasonic bath of acetone (5 min) and ethanol (5 min), and dried at 120 °C and 10^{-6} mbar for 0.5 h. Before OMBD, **1** was ground into a fine powder, and degassed at 120 °C and 10^{-9} mbar for 15 h. During OMBD, the base pressure in the chamber was 5×10^{-9} mbar, and the evaporation and substrate temperatures were 200 °C and 30 °C. The deposition rate was (5.0 ± 0.5) nm min^{-1}. The thickness of the films was in-situ controlled by a quartz microbalance, calibrated by ellipsometry, atomic force microscopy, and α-step measurements. The films appeared transparent and homogeneous. The absorption spectra showed that the films were transparent in the range 400–2000 nm. The absorption maximum (λ_{max}) was at 363 nm, and the cut-off edge (90 % transmission) at about 400 nm.

We used scanning electron microscopy (SEM) to study the surface morphology of a film of **1** grown on an amorphous glass substrate at 100 °C (Fig. 2). At such a high substrate temperature (T_s = 0.65 T_m), normal low molecular weight organic materials are expected to easily crystallize into micrometer-sized crystallites due to high mobility of the molecules, leading to high scattering losses within the film. For the supramolecular assemblies **1**, however, the film appeared featureless (Fig. 2). Its roughness (root mean square value, RMS) was 5 ± 3 nm as measured by atomic force microscopy. This value is smaller than the substrate roughness. Even though the film may consist of crystallites, their sizes appear smaller than 100 nm (Fig. 2), hence the scattering losses should be significantly lower than that in most organic polycrystalline films.

In order to determine the structural order of the films, X-ray diffraction in both reflection and transmission mode has been performed. The measurements cover the source materials (sublimated and unsublimated **1**), and thin films grown on glass, fused silica and silicon substrates. The main peak in the $\theta/2\theta$ scan was always found at 2θ = 24.9° (d = 3.57 Å). For the thin films deposited on glass substrates, we have only found this main peak with a large half width. For a 400 nm thick film of **1** deposited at a substrate temperature of 30 °C, for example, the full width at half

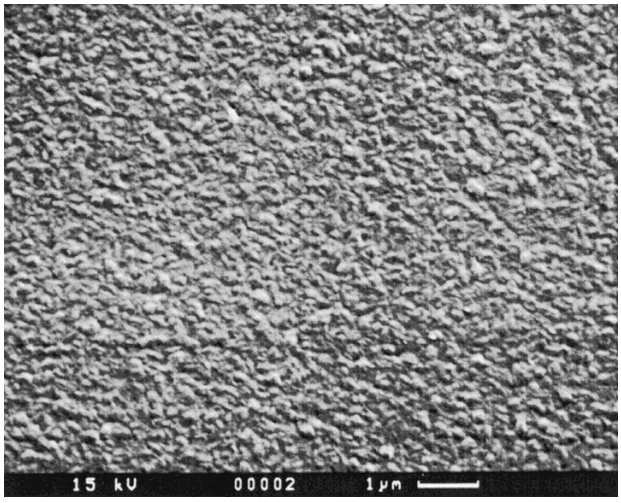

Fig. 2. SEM image (scale bar at the bottom: 1 μm) of a film of **1** grown on an amorphous glass substrate at 100 °C. To prevent sample charging, the film is covered with a 5 Å Pt layer.

maximum corresponds to 0.841°. Assuming that this broadening is only due to particle size, the average particle dimension is about 10 nm, according to the Scherrer formula. However, this is not in agreement with the results of our solid state ^{15}N NMR studies of the sublimated samples, which show no sign of the free pyridyl group, that is, the molecules are mostly (>99 %) head-to-tail hydrogen bonded to long chains. Another more likely explanation for this broadening could be a disturbed stacking sequence perpendicular to the substrate surface. In the Laue transmission experiments with white radiation (U_{max} = 40 kV), we were not able to observe any reflections, nor even with long exposure times (>24 h) or grazing incidence of the X-ray beam. Instead, we observed strong radiation damages of the glass substrate in contrast to the reflection measurement carried out with much lower energy $E \approx 10$ keV. In order to obtain more information on the structure of the thin films, we now study their nonlinear optical properties.

Since **1** is hardly soluble in common organic solvents, it was not possible to measure its molecular second-order polarizability (β) by electric field-induced second-harmonic generation (EFISH)[1] and hyper-Rayleigh scattering.[1] Semiempirical calculation was then performed using the MOPAC Hamiltonian (AM1, Cerius^2, Molecular Simulations Inc.). The results indicate that the second-order polarizability of the linear polymer of **1** is dominated by its tensor component along the long molecular axis (β_{zzz}). This implies that the molecule has a significant hyperpolarizability only for light polarized along the long axis of the molecule. For the bulk material, the induced second harmonic polarization that radiates the second harmonic light is given[1] by $P^{2\omega}{}_i = \varepsilon_0\, d_{ijk} E^{\omega}{}_j E^{\omega}{}_k$ (the Einstein summation convention applies), where d_{ijk} is the second order susceptibility tensor, $E^{\omega}{}_j$ is the electric field vector component of the fundamental wave along the j axis, $P^{2\omega}{}_i$ is the second harmonic polarization component along the i axis, and ε_0 is the

  0935-9648/99/0906-0747 $ 17.50+.50/0

permittivity of vacuum. If the molecules in a film are preferentially oriented along an axis, denoted as the X'_3 axis, d_{ijk} of the film then possesses a large d_{333} component, and only a small d_{311} component. Assuming a loss-less material, Kleinmann symmetry dictates $d_{311} = d_{131} = d_{113}$; while d_{111}, d_{331}, d_{313}, and d_{133} should be zero.

The second harmonic generation (SHG) experiments were performed in transmission mode using a BMI Nd:YAG laser delivering 7 ns long pulses at a wavelength of 1064 nm at a repetition rate of 10 Hz. The second harmonic signal of the films as a function of the incident angles Θ is shown in Figure 3A. The second harmonic intensity $I^{2\omega} \approx (I^{\omega})^2$ reaches its maximum when the fundamental polarization is parallel to the substrate plane (incident fundamental ray perpendicular to the substrate). This is expected when the ordering direction of the film is parallel to the substrate surface.

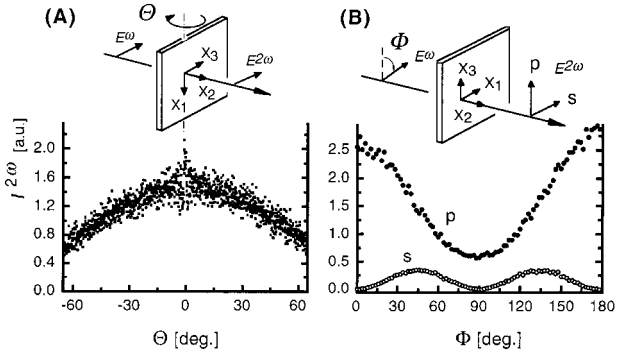

Fig. 3. SHG intensity ($I^{2\omega}$) as a function of the incident angle Θ (A) and polarization angle Φ (B) of the fundamental (λ_0 = 1064 nm) incident on a 200 nm thick film of **1** grown on a glass substrate at 30 °C by OMBD. The deposition coordinates $\{X_1, X_2, X_3\}$ are defined as follows: X_3 is the projection of the molecular beam on the substrate surface; X_2 is the surface normal and rotation axis for (B); X_1 is perpendicular to both X_2 and X_3, and is the rotation axis for (A). $\Theta = 0$ or $\Phi = 0$ denotes that both E^{ω} and $E^{2\omega}$ are parallel to X_3. The curves are typical for all films of **1** grown under similar conditions. The scattering of data at $\Theta = 0$ and $\Phi = 0$ is due to multiple reflections.

Figure 3B shows the influence of the polarization angle Φ of the fundamental wave on the components of the second harmonic signal with polarization parallel (p) and perpendicular (s) to the X_3 direction. For a film with a preferential transition dipole orientation parallel to the substrate surface, the second harmonic polarization components are given by

$$P^{2\omega}{}_3(\Theta = 0°, \Phi) = \varepsilon_0\, d_{333} \cos^2(\Phi) + d_{311} \sin^2(\Phi) \quad (1)$$

$$P^{2\omega}{}_1(\Theta = 0°, \Phi) = 2\, \varepsilon_0\, d_{113} \cos(\Phi) \sin(\Phi) = \varepsilon_0\, d_{113} \cos(2\Phi) \quad (2)$$

The second harmonic signal detected in the experiment is proportional to the square of the second harmonic polarization amplitude $P^{2\omega}$. The signal due to the polarization component $P^{2\omega}{}_3$ along X_3 follows the dependence predicted by Eq. (1). Since we know from the previous measurement that the preferential molecular direction is parallel to the substrate, we conclude that the contribution of the largest nonlinear-optical coefficient d_{333} corresponds to the maximum of the curve and the contribution from the small d_{311} coefficient corresponds to the minimum. We also see that the signal due to $P^{2\omega}{}_1$ (signal polarization along X_1) oscillates twice as fast as a function of Φ, as predicted by Eq. (2), with the contribution of $d_{113} \approx d_{311}$ corresponding to the maximum of the curve. Since $P^{2\omega}{}_3$ has its maximum for $\Phi = 0$, the contribution of d_{333} is obtained when both fundamental and second harmonic waves are polarized along X_3, which is therefore the direction along which the long molecular axes are preferentially oriented.

These measurements prove that the molecules are preferentially aligned along the projection of the molecular beam direction on the substrate surface (the X_3 axis). This alignment direction was the same as that of the films of **2**, and was confirmed by repeated experiments. It is dependent on the deposition coordinates depicted in Figure 3, but not on the rotation angle of the substrate around its surface normal (the X_2 axis) during the deposition. Therefore, using such supramolecular assemblies and oblique incidence OMBD, one can in-situ orient the film anisotropy to any desired in-plane direction relative to the substrate edges simply by choosing the angle between the substrate edges and the projection of the molecular beam on the substrate.

The second harmonic intensities ($I^{2\omega}$) at different regions of the large films (2×2 cm^2) varied within 10 %, which was within the experimental error, indicating a high homogeneity of the film over the large area. In addition, the second harmonic intensity $I^{2\omega}$ increased quadratically with the film thickness (Fig. 4). This behavior is characteristic for films having a uniform non-centrosymmetric order that does not decrease with increasing film thickness.[21] The strong hydrogen bonding between molecules of **1** is expected to stabilize this order. Indeed, the SHG intensity only slightly decreased before the temperature reached 190 °C (Fig. 5). On the other hand, $I^{2\omega}$ of the films of **2** diminished rapidly starting from 180 °C. Therefore, the thermal stability of the films of **1** is higher than that of the films of **2**, probably related to the higher melting point of **1** (350 °C) than **2** (300 °C).

The nonlinear optical coefficient (d_{33}) of 0.55 ± 0.05 pm V^{-1} was obtained from the Maker-fringe method[22] at the fundamental λ_0 = 1064 nm, calibrated with a quartz reference (d_{11} = 0.3 pm V^{-1}). There was no overlap of the second harmonic ($\lambda_{2\omega}$ = 532 nm) and the absorption charge transfer band of the films (λ_{max} = 363 nm), hence resonance enhancement can be neglected. This value was lower than that of the films of **2** (d_{33} = 0.75 ± 0.07 pm V^{-1}), probably due to the less linear and rigid structure of **1** than **2**. The nonlinear optical coefficients may be increased by an appropriate choice of deposition angle (the angle between the molecular beam direction and the substrate normal). Unfortunately, due to our chamber design we were not able to change this angle. We have started to perform experiments in a different UHV system**.** Preliminary results show

  0935-9648/99/0906-0748 $ 17.50+.50/0

ADVANCED MATERIALS

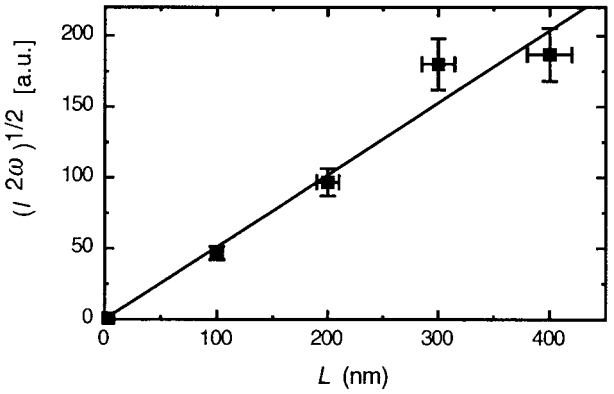

Fig. 4. Square root of the SHG intensity $[(I^{2\omega})^{1/2}]$ for films of **1** grown on glass substrates at 30 °C by OMBD as a function of the film thickness (L). The straight line is the linear least-squares fit to the experimental data. Fundamental light of $\lambda_0 = 1064$ nm was used.

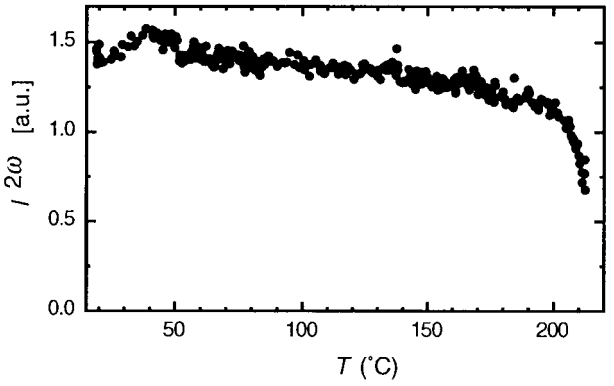

Fig. 5. SHG intensity ($I^{2\omega}$) for a 200 nm film of **1** grown on glass at 30 °C by OMBD as a function of temperature (T) with a heating rate of 7.2 K min^{-1}. Fundamental light of $\lambda_0 = 1064$ nm was used.

4.4 times and 6.8 times increase in the d_{33} value by changing the deposition angle from 10° to 20°, and to 30°.

In conclusion, we have proposed a new type of organic nonlinear optical material: amorphous supramolecular polymers of small molecules that are linked in a head-to-tail arrangement via strong hydrogen bonding. Such materials can be sublimed, and they self-assemble or polymerize again in a head-to-tail arrangement. Therefore, they are particularly suitable for growth of thin films by OMBD. This novel approach to grow NLO-active organic thin films was demonstrated with model compounds **1** and **2**, showing that it is possible to preferentially orient the molecules to any desired direction within the substrate plane by oblique OMBD. Hence, this technique can be used to fabricate, for example, stacked organic layers of the same molecules but varied orientations. This can be easily done by rotating the substrate around its normal during deposition. For nonlinear optics, it is possible to deposit waveguides with periodic modulation in the sign of the nonlinearity by using masks and turning the substrate by 180° between deposition steps. Such structures can be designed to allow efficient nonlinear interaction at almost any wavelength through the well-known quasi-phase matching process. Moreover, the ordering of the films was thermally stable and did not decrease with increasing film thickness at least up to 400 nm. Although the nonlinear optical coefficient (d_{33}) of these films is still too low for practical applications, the results reported in this and the subsequent paper provide a hint on how to increase this value by optimization of the materials and deposition conditions.

Experimental

4-[*trans*-(Pyridin-4-ylethenyl)]benzoic acid (**1**) was prepared according to [23]. The crude product (light yellow powder) was purified by precipitation from hot pyridine to give a white powder. The product was hardly soluble in H_2O, MeOH, DMF, $CHCl_3$ etc., and slightly soluble in hot DMSO. ^{1}H NMR and electron ionization mass spectra of the product and its sublimate either from low vacuum (0.01 mbar) or from UHV (10^{-9} mbar) were identical. ^{1}H NMR (300 MHz, potassium salt in 5 mM KOH/D_2O): 8.29 (d, J = 6.2 Hz, 2 H); 7.77 (d, J = 8.3 Hz, 2 H); 7.45 (d, J = 8.7 Hz, 2 H); 7.30 (d, J = 6.2 Hz, 2 H); 7.20 (d, J = 16.6 Hz, 1 H); 6.94 (d, J = 16.2 Hz, 1 H). EI MS m/z (%): 225 (100, M^+), 180 (67, $[M-HCO_2]^+$). Anal. calc. for $C_{14}H_{11}NO_2$ (225.25): C 74.65, H 4.92, N 6.22; found: C 74.57, H 4.74, N 6.21. M.p. 350 °C (decomposed, measured by DSC with a scan rate of 5 K min^{-1}).

Received: September 21, 1998
Final version: March 5, 1999

[1] C. Bosshard, K Sutter, P. Prêtre, J. Hulliger, M. Flörsheimer, P. Kaatz, P. Günter, *Organic Nonlinear Optical Materials*, Gordon & Breach, Amsterdam **1995**.
[2] F. Kajzar, J. D. Swalen, Eds. *Organic Thin Films for Waveguiding Nonlinear Optics*, Gordon & Breach, Amsterdam **1996**.
[3] T. Dietrich, R. Schlesser, B. Erler, A. Kündig, Z. Sitar, P. Günter, *J. Crystal Growth*, **1997**, *172*, 473.
[4] J. Lemoigne, in *Organic Thin Films for Waveguiding Nonlinear Optics* (Eds: F. Kajzar, J. D. Swalen), Gordon & Breach, Amsterdam **1996**, Ch. 7, p. 289.
[5] P. A. Chollet, Y. Levy, in *Organic Thin Films for Waveguiding Nonlinear Optics* (Eds: F. Kajzar, J. D. Swalen), Gordon & Breach, Amsterdam **1996**, Ch. 9, p. 457.
[6] G. Decher, B. Tieke, C. Bosshard, P. Günter, *Ferroelectrics* **1989**, *91*, 193.
[7] C. Bosshard, M. Küpfer, in *Organic Thin Films for Waveguiding Nonlinear Optics* (Eds: F. Kajzar, J. D. Swalen), Gordon & Breach, Amsterdam **1996**, Ch. 4, p. 163.
[8] S. R. Forrest, *Chem. Rev.* **1997**, *97*, 1793.
[9] A. Ulman. *Chem. Rev.* **1996**, *96*, 1533.
[10] C. M. Bell, H. C. Yang, T. E. Mallouk, in *Materials Chemistry of Organic Monolayer and Multilayer Thin Films* (Eds: L. V. Interrante, L. A. Caspar, A. B. Ellis), Am. Chem. Soc., Washington, DC **1995**, Ch. 8, p. 211.
[11] J. Salbeck, *Ber. Bunsen-Ges. Phys.* **1996**, *100*, 1667.
[12] M. Thelakkat, H. W. Schmidt, *Adv. Mater.* **1998**, *10*, 219.
[13] J. M. Lehn, *Makromol. Chem., Macromol. Symp.* **1993**, *69*, 1.
[14] R. P. Sijbesma, F. H. Beijer, L. Brunsveld, B. J. B. Folmer, J. Hirschberg, R. F. M. Lange, J. K. L. Lowe, E. W. Meijer, *Science*, **1997**, *278*, 1601.
[15] F. Takusagawa, A. Shimada, *Acta Crystallogr.* **1976**, *B32*, 1925.
[16] a) C. Cai, M. M. Bösch, Y. Tao, B. Müller, Z. Gan, A. Kündig, C. Bosshard, I. Liakatas, M. Jäger, P. Günter, *J. Am. Chem. Soc.* **1998**, *120*, 8563. b) B. Müller, C. Cai, M. Bösch, M. Jäger, C. Bosshard, P. Günter, J. V. Barth, J. Weckesser, K. Kern, *Thin Solid Films* **1999**, *343–344*, 165.
[17] L. Ukrainczyk, K. A. Smith, *Environ. Sci. Technol.* **1996**, *30*, 3167, and refs cited therein.
[18] J. Schaefer, E. O. Stejskal, *J. Am. Chem. Soc.* **1976**, *98*, 1031.
[19] W. Städeli, W. Philipsborn, *Org. Magn. Reson.* **1981**, *15*, 106.
[20] M. Kiguchi, M. Kato, M. Okunaka, Y. Taniguchi, *Appl. Phys. Lett.* **1992**, *60*, 1933.
[21] W. Lin, W. Lin, G. K. Wong, T. J. Marks, *J. Am. Chem. Soc.* **1996**, *118*, 8034.
[22] J. Jerphagnon, S. K. Kurtz, *J. Appl. Phys.* **1970**, *41*, 1667.
[23] G. Drefahl, E. Gerlach, *J. Prakt. Chem.* **1958**, *4*, 72.

  0935-9648/99/0906-0749 $ 17.50+.50/0